Keggin Ions

$[SiNb_{12}O_{40}]^{16-}$ and $[GeNb_{12}O_{40}]^{16-}$: Highly Charged Keggin Ions with Sticky Surfaces**

May Nyman, François Bonhomme, Todd M. Alam, John B. Parise, and Gavin M. B. Vaughan*

Heteropolyanions are negatively charged clusters of corner-sharing and edge-sharing early transition-metal MO_6 octahedra and heteroatom XO_4 tetrahedra, in which the tetrahedra are usually located in the interior of the cluster.[1] The geometry, composition, and charge of these clusters are varied through synthesis parameters, and cluster properties are highly tunable as a function of these characteristics. Heteropolyanions have been employed in a range of applications that include virus-binding inorganic drugs,[2] homogeneous and heterogeneous catalysts,[3,4] electro-optic and electrochromic materials,[5,6] metal and protein binding,[7] and as building blocks for nanostructuring of materials.[8] The α-Keggin geometry, which was first structurally characterized in 1933 by J. F. Keggin[9] for the phosphotungstic acid ($H_3PW_{12}O_{40}$) is one of the most widely recognized and thoroughly studied heteropolyanion geometries.[10] Following Keggin's initial discovery, solid-state and solution chemistries of the heteropolytungstates and heteropolymolybdates (i.e., $H_4SiMo_{12}O_{40}$) with the Keggin geometry have been well developed. These Keggin ions have been synthesized with a variety of atoms in the XO_4 tetrahedral site, numerous addenda atom substitutions in the MO_6 octahedral sites, as acids, and as salt compounds with a range of counter cations.[11,12] Given the apparent ubiquity of the Keggin geometry, it is not surprising that the first-observed heteropolyniobate (reported Nyman et al. in 2002[13]) was a Keggin ion. However, we first identified[13] the $[SiNb_{12}O_{40}]^{16-}$ α-Keggin ion in the solid state as a 1D inorganic polymer that features alternating Nb-Keggin ions and $[Ti_2O_2]^{4+}$ bridges, rather than isolated clusters. Presented here is the first synthesis and structural characterization of the dodecaniobate Keggin ion in the form of a water-soluble salt that contains isolated clusters. Solution and solid-state multinuclear NMR spectroscopies were used to better characterize the relationship between the solid-state structure and solution behavior of these highly charged species. To our knowledge, the $[TNb_{12}O_{40}]^{16-}$ (T = Si, Ge) Keggin ions reported herein have the highest negative charge observed for clusters that have the plenary Keggin geometry; and also higher charge than the typical mono-, bi- and trivacant lacunary Keggin ions. The unprecedented high charge should render these clusters unique with regard to metal binding and other applications that involve anion–cation electrostatic interactions in solution or at interfaces.

These $[TNb_{12}O_{40}]^{16-}$ clusters (T = Si, Ge): $Na_{16}[SiNb_{12}O_{40}]\cdot 4H_2O$ **1**; $Na_{16}[GeNb_{12}O_{40}]\cdot 4H_2O$ **2** are chemically quite different from the related heteropolymolybdate and heteropolytungstate Keggin ions in their synthetic approach, their pH stability, and their charge. The Nb Keggin ions are synthesized and stable in basic solutions (pH 7–12.5) and decompose in acidic solutions, whereas the Mo and W Keggin ions are synthesized and stable in acidic solutions (pH ≈ 1–3) and decompose in more basic solutions. The Nb Keggin ions are synthesized hydrothermally at 190 °C from amorphous, hydrous niobium oxide and alkoxides of germanium or silicon, whereas the Mo and W Keggin ions are generally precipitated at room temperature from tungstic or molybdic acid or alkali precursors. Use of sodium silicate or sodium germanate as precursors rather than the alkoxides results in mixtures that contain the heteropolyniobate only as a minor phase, with poorly crystalline sodium niobates[14] as the major phase. The general differences between synthesis of heteropolyniobates and synthesis of heteropolymolybdates and heteropolytungstates have been discussed in detail previously.[13] The hydrothermal formation of $Na_{16}[TNb_{12}O_{40}]\cdot 4H_2O$ (T = Si, Ge) is quite sensitive to processing parameters. Time-dependent investigations of the synthetic pathway of the Nb Keggin ion revealed that after 1 hour of

[*] Dr. M. Nyman, Dr. F. Bonhomme
Sandia National Laboratories
Department of Geochemistry
Albuquerque, NM 87185 (USA)
Fax: (+1) 505-844-7354
E-mail: mdnyman@sandia.gov
Dr. T. M. Alam
Sandia National Laboratories
Department of Organic Materials
Albuquerque, NM 87185 (USA)
Prof. Dr. J. B. Parise
Center for Environmental Molecular Sciences
Department of Geosciences
Chemistry Department
State University of New York
Stony Brook, NY 11794–2100 (USA)
Dr. G. M. B. Vaughan
Materials Science, European Synchrotron Radiation Facility, BP 220, 38043 Grenoble CEDEX (France)

[**] This work was supported by Sandia's Laboratory Directed Research and Development (LDRD) Program. Sandia is a multiprogram laboratory operated by Sandia Corporation, a Lockheed Martin Company, for the United States Department of Energy under Contract DE-AC04–94AL85000. We thank Reference Metals Co., Inc. (Bridgeville, PA) for contribution of hydrous niobium oxide. J.B.P. acknowledges support of the NSF.

 DOI: 10.1002/ange.200353410

hydrothermal treatment at 180 °C, the Lindqvist ion, $Na_7(H_3O)^+[Nb_6O_{19}]\cdot 14\,H_2O$,[15] is precipitated. After 2 h, a clear solution is observed with all solids dissolved, and 3 h results in the Nb Keggin ion salt as the only crystalline phase. Yet, if the Lindqvist ion is used as the niobium precursor (with a 1:1 molar replacement of Nb), 1D Nb Keggin chain materials (unpublished results) are the major products of hydrothermal processing. However, if either NaOH or NaCl is added to this Lindqvist ion reaction, the product is again the isolated Nb Keggin clusters, which suggests the common-ion effect plays a role in these syntheses. In the case of the synthesis of the silicon analogue, a slight decrease in NaOH concentration in the precursor solution results in the formation of a different cluster geometry with the composition $Na_{14}[H_2Si_4Nb_{16}O_{56}]\cdot 45.5\,H_2O$.[13]

From the microcrystalline powder of **1**, an approximately cube-shaped crystal with a diameter of 15 μm was selected for single-crystal X-ray diffraction analysis at the European Synchrotron Radiation Facility (ESRF).[16] The structure of **1** was solved in the cubic space group, $P\bar{4}3n$. Rietveld refinement (program Fullprof2K[17]) of the diffraction patterns of **1** and **2**, based on the results from a single crystal, confirmed that the single crystal is representative of the bulk microcrystalline powders, that no crystalline impurities are present, and that **1** and **2** are isostructural. The X-ray powder-diffraction spectra of **1** and **2**, along with the difference pattern between the observed X-ray powder data for **1** and the diffraction pattern calculated from the single-crystal structure of **1** are shown in Figure 1. The lattice constants of

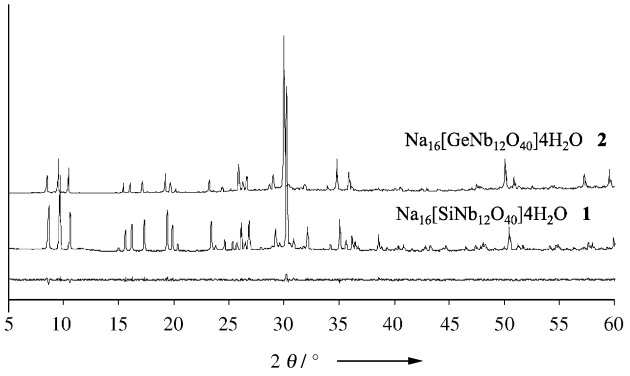

Figure 1. Observed powder X-ray diffraction patterns of **1** and **2**, and difference between the diffraction pattern calculated from single-crystal data and observed X-ray powder data of **1**.

1 and **2** were refined from powder-diffraction data by using the Le Bail method,[18] with silicon SRM640 from the National Institute of Standards and Technology (NIST) as internal standard: **1** $a = 20.4875(2)$ Å, **2** $a = 20.5349(4)$ Å. The single-crystal data of **1** reveals two crystallographically distinct $[SiNb_{12}O_{40}]^{16-}$ α-Keggin ions in the unit cell. Keggin 1 resides at the origin and in the center of the cubic cell and pairs of Keggin 2 are located on the faces of the unit cell, giving a 1:3 ratio of Keggin 1 to Keggin 2. Figure 2 shows the two Keggin ions in a ball-and-stick model. The $Nb1O_6$ octahedra of Keggin 1 and the $Nb2O_6$, $Nb3O_6$, and $Nb4O_6$

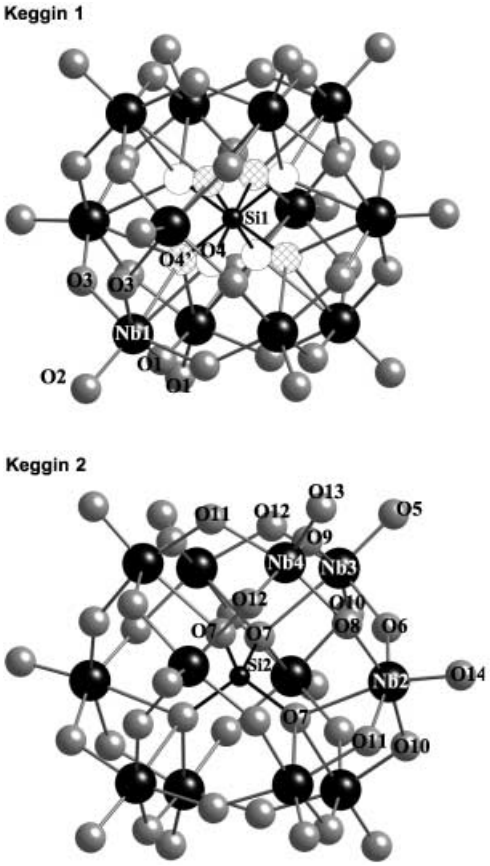

Figure 2. Ball-and-stick representation of the two crystallographically unique Keggin ions of **1**. Bond lengths [Å] of Keggin 1 (top), O4 and O4′ are half occupied: Si1–O4 1.62(2), Si1–O4′ 1.60(2), Nb1-O2 1.735(9), Nb1-O3a 1.92(1), Nb1-O3 1.94(1), Nb1-O1 1.97(1), Nb1–O4 2.46(1), Nb1–O4′ 2.49(1). Bond lengths [Å] of Keggin 2 (bottom): Si2-O7 1.659(7), Nb2-O14 1.778(8), Nb2-O6 1.937(8), Nb2-O8 1.953(7), Nb2-O10 1.995(8), Nb2-O11 2.026(8), Nb2-O7 2.395(7), Nb3-O5 1.765(9), Nb3-O10 1.976(8), Nb3-O9 1.981(8), Nb3-O6 1.991(8), Nb3-O12 2.03(1), Nb3-O7 2.408(7), Nb4-O13 1.765(8), Nb4-O9 1.975(8), Nb4-O12 1.987(9), Nb4-O8 2.003(7), Nb4-O11 1.998(8).

octahedra of Keggin 2 are distorted in the regular fashion of polyoxometalate d^0 metal centers with a long axial Nb–O_c bond to the center of the cluster (2.395(7)–2.49(1) Å), a short axial Nb–O_t terminal bond (ranging from 1.735(9) to 1.778(8) Å) to the outside of the cluster, and four intermediate equatorial Nb–O_b bonds (between 1.92(1) and 2.03(1) Å). Sixteen sodium atoms per cluster were located from the single-crystal data of **1**, which is the necessary amount to balance the charges of the cluster. Bond-valence sum calculations (BVS)[19] for the oxygen atoms of the clusters ruled out the presence of protons bonded to the Keggin oxygen atoms.

The ratio of Keggin 1 to Keggin 2 in **1** was confirmed by solid-state ^{29}Si MAS NMR spectroscopy. The ^{29}Si MAS NMR spectrum (Figure 3) shows a signal at −74.1 ppm (77 %) with a shoulder at −72.6 ppm (23 %) which is in agreement with a 3:1 ratio of the two Keggin ions. The $Si1O_4$ tetrahedron of Keggin 1 is disordered with Si1 surrounded by eight half-occupied oxygen atoms (O4 and O4′ sites). The Si1–O4 bond length is 1.62(2) Å and the Si1–O4′ bond length is 1.60(2) Å.

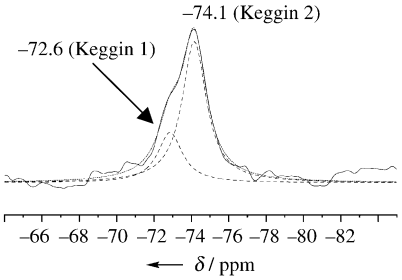

Figure 3. Solid-state ^{29}Si MAS NMR spectrum of $Na_{16}[SiNb_{12}O_{40}]\cdot 4\,H_2O$ **1**. The spectral deconvolution of the overlapping resonances is shown. The two resolvable peaks are assigned to $Si1O_4$ and $Si2O_4$ of Keggin 1 and Keggin 2, respectively.

In Keggin 2, Si2 is tetrahedrally bound to four O7 atoms, with a bond length of 1.659(7) Å. Therefore these two sites are distinguishable by ^{29}Si NMR based on the slight difference in geometry of the SiO_4 tetrahedra. In solid-state structures, ^{29}Si signals shift downfield with both increasing Si–O bond length[20] and increasing Si-O-X bond angle.[21] Both Si-O-Nb bond angle and Si–O bond length are slightly larger for Keggin 2, which confirms the ^{29}Si NMR assignment based on the ratio of the resonances.

The ^{17}O solid-state NMR spectrum of the germanium analogue **2** (Figure 4) shows two distinct environments for oxygen atoms (O_c) bonded to the central tetrahedral germanium, but the solid-state ^{17}O spectrum of the Si-analogue **1** clearly shows a single O_c site. The ^{17}O MAS NMR spectroscopic experiments were run at different magnetic-field strengths to prove the two O_c peaks of **2** are not a result of a second-order quadrupolar-broadening effect. These data suggest that the O_c sites of Keggin 1 (O4, O4′) and Keggin 2 (O7) are more similar in the Si analogue than in the Ge analogue. The two solid-state ^{17}O peaks for the O_c positions of **2** become a single peak in solution, and the O_c peak for **1** remains a single peak in solution (see Figure 4 and Table 1). The O_c signals of **1** and **2** have approximately the same chemical shift in solution. The O_c signal of **1** does not shift significantly upon dissolution, whereas the two O_c peaks of **2** undergo a downfield shift of around 15 and 30 ppm, respectively. Since we do not have a single-crystal structure of **2**, the differences in O_c geometry between **1** and **2** cannot be quantitatively described. However, it is likely to be related to the difference between Ge–O and Si–O bond lengths (Ge–O bond lengths typically exceed Si–O bond lengths by about 0.1 Å), and how these T–O bonds are affected by packing distortions in the solid state. The packing distortions are eliminated in solution since the two O_c resonances of the Ge analogue becomes a single signal. An explanation for this would be that the cluster geometry becomes more flexible upon dissolution, or that a fluxional molecular rearrangement occurs. The atoms within the clusters are allowed to "relax" to optimum coordination geometries, which may not necessarily be the same constrained geometries in the solid-state lattice.

The ^{17}O and ^{23}Na NMR spectroscopic analyses provide evidence that **1** and **2** display an unusual behavior of strongly associating with their charge-balancing cations upon dissolution, and these results are described in the following

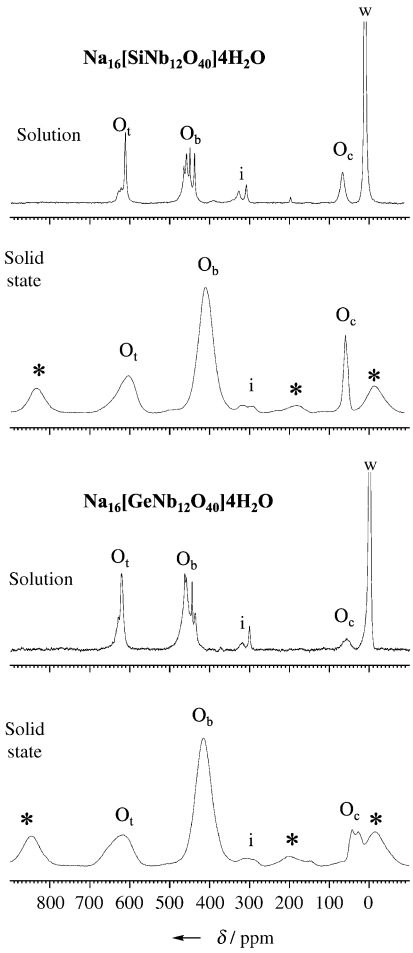

Figure 4. Solid-state and solution ^{17}O NMR spectra of isotopically enriched $Na_{16}[SiNb_{12}O_{40}]\cdot 4\,H_2O$ (left) and $Na_{16}[GeNb_{12}O_{40}]\cdot 4\,H_2O$ (right). O_t, O_b, and O_c are terminal, bridging, and central oxygen atoms. Spinning sidebands are marked with *; signals identified as impurities are marked with i (sodium carbonate and niobium oxide) w is water oxygen. The assignments of the solid-state and solution ^{17}O O_t, O_b, and O_c signals were made based on the previous NMR spectroscopic studies on the molybdate and tungstate Keggin ions.[25–28]

Table 1: ^{17}O NMR spectroscopic chemical shifts for **1** and **2** in the solid state and solution

Sample	δ [ppm]		
	O_t[a]	O_b[a]	O_c[a]
$Na_{16}[GeNb_{12}O_{40}]\cdot 4\,H_2O$ (**2**)	609	415	43
solid-state	643		26
$Na_{16}[GeNb_{12}O_{40}]\cdot 4\,H_2O$ (**2**)	621.3	437.3	57.3
solution	629.4	444.7	
		459.4	
		463.1	
$Na_{16}[SiNb_{12}O_{40}]\cdot 4\,H_2O$ (**1**)	601	406	50
solid-state	636		
$Na_{16}[SiNb_{12}O_{40}]\cdot 4\,H_2O$ (**1**)	608.6	433.0	56.9
solution	625.1	444.4	
	619.3	452.8	
		459.9	

[a] Compared to H_2O, 0 ppm.

discussions. In the solid state, the sodium atoms (16 per cluster) reside between the Keggin clusters, and each sodium atom bridges at least two separate Keggin ions. This arrangement lends a structural resemblance to a 3D network of linked Keggin ions. Keggin 1 has 30 Na atoms bonded to its terminal and bridging oxygen atoms with a total of 60 Na–O bonds; and Keggin 2 is bonded to 38 Na atoms through 74 Na–O bonds (all Na–O bonds are between 2.3–2.7 Å). Figure 5 emphasizes this bonding between the sodium and

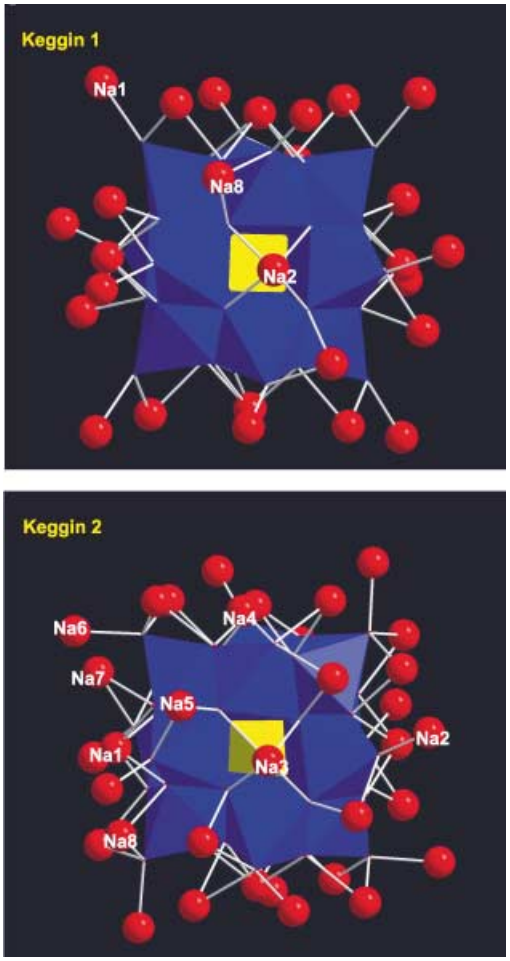

Figure 5. Polyhedral representation of Keggin 1 (top) and Keggin 2 (bottom), showing the sodium ion bound to the surface in the solid state (red spheres).

Keggin ions in the solid state. In conjunction with the extensive binding between the Na cations and the anionic cluster in the solid state, this crystal lattice contains remarkably few water molecules: only four water molecules per cluster, or 0.25 per Na cation. Normally, lattices of the Nb-based polyoxometalate salts,[13,15,22–24] as well as those of the polyoxotungstates and polyoxomolybdates,[1] carry 15–50+ water molecules per cluster that both solvate the charge-balancing cations and hydrogen bond to the oxygen atoms of the cluster. This unusual feature of strong binding between the sodium atoms and the anionic Keggin clusters observed here is likely to be related to stabilization of the high surface charge of the clusters. Furthermore, the arrangement of the Keggin ion oxygen atoms apparently provides good coordination sites for metal cations. For instance, every "four-ring window" of Keggin 1 and Keggin 2 hosts a sodium cation in a cryptate-like fashion (see Figure 5, Na1, Na2, and Na3).

The ^{17}O solution and solid-state spectra of **1** and **2** are compared in Figure 4. As observed for the related molybdates and tungstates, the signals of the solid-state ^{17}O spectra are sufficiently broadened so that only one signal position is identified for the O_t), O_b, and O_c sites (with the exception of the O_c site of **2**, discussed above). The surprising result of the ^{17}O solution experiments is the number of resolvable peaks in the spectral region of terminal and bridging oxygen atoms for **1** and **2** (see Table 1). Based on similar work on the related molybdates and tungstates, we expected to see only two peaks for the bridging oxygen atoms;[25–28] one for the μ_2-O bridging two edge-sharing NbO_6 octahedra and one for the μ_2-O bridging two corner-sharing NbO_6 octahedra. Yet we observe four signals. Furthermore, we anticipated only one signal for the terminal oxygen, rather than two or three that are observed. The splitting of the O_t and O_b ^{17}O solution NMR spectroscopic signals is attributed to symmetry-reducing distortions of the clusters. The biggest contribution to distortion of the terminal and bridging oxygen sites of Keggin 1 and Keggin 2 of **1** and **2** in the solid state is likely to be binding of the clusters to sodium in the crystal lattice, thus resulting in differences in bond angles and lengths about the oxygen atoms. However, we expect these differences to be eliminated upon dissolution if the clusters were to shed their bound sodium cations. This is clearly not the case, given the number of resolvable oxygen sites observed by solution ^{17}O NMR. Therefore, this peak splitting can be attributed to the retention of cluster-bound sodium atoms in solution, and perhaps also dissolution of **1** and **2** as small oligomeric units, linked together by the bound sodium atoms.

Solution ^{23}Na NMR spectroscopy provided further evidence for this solution behavior of the Nb Keggin ions. The ^{23}Na NMR spectra of three different solution concentrations of **1**, and the same three solution concentrations of $Na_7H_3O^+[Nb_6O_{19}]\cdot 14\,H_2O$[15] normalized to sodium concentration were analyzed (see Table 2). The hexaniobate Lindqvist ion was used for comparison because it has a similar Na:Nb ratio as **1**, an equal negative charge per NbO_6 octahedron (−1.33), and similar solution pH to concentration correlation.

Table 2: Solution ^{23}Na NMR spectroscopy of $Na_{16}[SiNb_{12}O_{40}]\cdot 4\,H_2O$ and $Na_7H_3O^+[Nb_6O_{19}]\cdot 14\,H_2O$

Concentration Na [ppm]	Solution pH	^{23}Na signal position [ppm][a]	Signal width [Hz, FWHM][a]
	$Na_{16}[SiNb_{12}O_{40}]\cdot 4\,H_2O$		
5	8.1	−0.27	23
50	9.4	−0.37	87
500	10.2	−0.69	242
	$Na_7H_3O^+[Nb_6O_{19}]\cdot 14\,H_2O$		
5	7.6	−0.17	16
50	9.5	−0.23	10
500	9.8	−0.01	16

[a] Compared to 1 M NaCl, 0 ppm, FWHM = 18.5 Hz.

The charge-balancing sodium atoms of the dissolved Lindqvist ion are clearly hydrated, in that the ^{23}Na resonance is narrow and close to 0 ppm, as expected for a water-soluble sodium salt. On the other hand, the resonance for the charge-balancing Na atoms of the Keggin ion shifts slightly and broadens significantly with increasing concentration of the dissolved cluster. The peak broadening is likely attributed to a dynamic equilibrium of the sodium ions between binding to the clusters and completely solvating in solution. Additionally the clusters may oligomerize in solution by linking through the sodium ions, as is observed in the solid-state structure. Both cluster linking and the degree of association of the sodium ions with the clusters is expected to increase with increasing solution concentration, which correlates with the increased peak broadening. Consistent with this observation, the ^{23}Na NMR resonances broadened upon cooling and sharpened with heating of the solution of **1**. However, resolution of different Na sites was not observed before reaching the freezing temperature of the solution.

With further study, the high negative charge of these new heteropolyniobates may be exploited for greater selectivity or strength of binding in applications that utilize the electrostatic interaction between negatively charged polyoxometalate clusters and positively charged species or species that feature positively charged regions (i.e., amino acids, proteins, metals, viruses). Additionally, a direct synthetic approach to $[TNb_{12}O_{40}]^{16-}$ makes substitutional variants between the niobate Keggin ion and heteropolyacids, such as the tungstate Keggin ion, potentially more attainable. The development of clusters with properties intermediate to the heteropolyacids and heteropolybases would allow access to highly tunable pH stability, charge, and composition. Therefore the introduction of these new basic and highly charged members to the Keggin family expands the potential of these greatly studied and applied materials.

Experimental Section

Synthesis of **1**: Sodium hydroxide (0.26 g, 6.5 mmol) was dissolved in water (8 mL) in the teflon liner of an autoclave. Amorphous $Nb_2O_5{\cdot}xH_2O$ (0.35 g, 2.0 mmol Nb–Nb precursor, 30 wt % water; Reference Metals Co. Inc., Bridgeville, PA) and tetraethylorthosilicate (0.27 g, 1.3 mmol) were added and the mixture was stirred for approximately 30 min. The pH of the precursor mixture was about 12.7. The teflon liner was loaded and sealed in a 23 mL stainless-steel autoclave, and heated at 190 °C for 12–24 h. The white, microcrystalline product was collected by filtration. Yield: 0.27 g $Na_{16}[SiNb_{12}O_{40}]{\cdot}4H_2O$, 0.12 mmol; 73 % based on Nb (Si is in excess).

Synthesis of **2**: Sodium hydroxide (0.16 g, 4.0 mmol) was dissolved in water (8 mL) in the teflon liner of an autoclave. Amorphous, hydrous $Nb_2O_5{\cdot}xH_2O$ (0.35 g, 2.0 mmol Nb; Reference Metals Co. Inc., Bridgeville, PA) and tetraethoxygermane (0.33 g, 1.3 mmol, Gelest, Inc.) were added and the mixture was stirred for approximately 30 min. The pH of the precursor mixture was about 11.5. The teflon liner was loaded and sealed in a 23 mL stainless-steel autoclave, and heated at 190 °C for 12–24 h. The white, microcrystalline product was collected by filtration. Yield = 0.20 g $Na_{16}[GeNb_{12}O_{40}]{\cdot}4H_2O$, 0.09 mmol; 53 % based on Nb (Ge is in excess).

X-ray powder diffraction of **1** and **2** was performed on a Bruker D8 Advance diffractometer in Bragg–Bretano geometry with Ni filtered $Cu_{K\alpha}$ radiation. Samples were prepared on a zero-background quartz plate and data were recorded from 5–90° with a step time of 25 s.

Elemental analysis: Elemental analysis was carried out on **1** by using an Perkin Elmer Elan 6100 ICP-MS. A solution of **1** was prepared by dissolving in DI water, diluting to an approximate concentration of 100 ppm of **1**, and acidifying with a small amount of nitric acid. Further dilutions to approximately 10 ppm and 1 ppm of **1** were made. Standards of Na, Si, and Nb were prepared by diluting 1000 ppm standards that had also been acidified with nitric acid. Results calcd (%):Nb 50.15, Na 16.15, Si 1.26; found: Nb 53.6, Na 15.7, Si 1.45.

The ^{17}O labeled samples of **1** and **2** were both produced by the identical reactions described above, except that they were scaled down by four and the solvent was 40.2 atom % ^{17}O water (Isotec, Inc., Miamisburg, Ohio).

The solid-state ^{17}O NMR MAS spectra were obtained on a Bruker Avance 600 instrument by using an observe frequency of 81.40 MHz, and a Bruker Avance 400 instrument with an observe frequency of 54.28 MHz. For the 81.40 MHz data the ^{17}O MAS NMR spectra were obtained by using a 2.5 mm broadband probe with spinning speeds between 30 and 35 kHz, with 2 μs π/6 pulses (π/2 pulse length 6 μs), 1 k scan averages and 5 s recycle delay. For the 54.28 MHz ^{17}O MAS NMR data and the ^{1}H–^{17}O cross-polarization (CP) MAS NMR data, a 4 mm broadband MAS probe spinning between 12.5 and 15 kHz was used. For all ^{17}O MAS NMR spectra high-power ^{1}H decoupling was employed by using the two-pulse phase modulation (TPPM) decoupling sequence.[29]

The solution ^{17}O NMR spectroscopic data were obtained on a Bruker Avance 600 instrument at 81.40 MHz by using a 5 mm broadband probe. The ^{17}O direct Bloch decay spectra were obtained by using a 0.5 s recycle delay, 8 μs π/2 pulses, 512 scan averages and ^{1}H decoupling. The ^{17}O NMR spectra were all referenced to external neat $H_2{}^{17}O$ ($\delta = 0.0$ ppm) at 25 °C.

The solid-state ^{29}Si MAS NMR spectra were obtained on a Bruker Avance 600 instrument by using an observe frequency of 119.2 MHz, a spinning speed of 5 kHz, and a single-pulse Bloch decay sequence with 1640 scan averages, 3 μs π/4 pulses, 240 s delay, with the spectra being referenced to a secondary external Q_8M_8 ($\delta = 12.4$ ppm) standard.

The solution ^{23}Na NMR spectra were obtained on a Bruker Avance 400 instrument using 100 scan averages, 6.75 μs π/2 pulses with a 10 ms recycle delay. The ^{23}Na chemical shifts were referenced to a secondary external 1M NaCl standard at RT ($\delta = 0.0$ ppm).

Received: November 26, 2003 [Z53410]

Keywords: hydrothermal synthesis · niobium · NMR spectroscopy · polyanions · polyoxometalates

[1] M. T. Pope, *Heteropoly and Isopoly Oxometalates*, Springer-Verlag, New York, **1983**.
[2] J. T. Rhule, C. L. Hill, D. A. Judd, *Chem. Rev.* **1998**, *98*, 327.
[3] I. V. Kozhevnikov, *Chem. Rev.* **1998**, *98*, 171.
[4] N. Mizuno, M. Misono, *Chem. Rev.* **1998**, *98*, 199.
[5] T. Yamase, *Chem. Rev.* **1998**, *98*, 307.
[6] M. Sadakane, E. Steckhan, *Chem. Rev.* **1998**, *98*, 219.
[7] D. E. Katsoulis, *Chem. Rev.* **1998**, *98*, 359.
[8] E. Coronado, C. J. Gomez-Garcia, *Chem. Rev.* **1998**, *98*, 273.
[9] J. F. Keggin, *Nature* **1933**, *131*, 908.
[10] Y. P. Jeannin, *Chem. Rev.* **1998**, *98*, 51.
[11] S. H. Wasfi, W. L. Johnson, *Synth. React. Inorg. Met.-Org. Chem.* **1999**, *29*, 697.
[12] H. T. Evans, in *Perspectives in Structural Chemistry*, *Vol. IV* (Eds.: J. D. Dunitz, J. A. Ibers), John Wiley & Sons, New York, **1971**, p. 7.

[13] M. Nyman, F. Bonhomme, T. M. Alam, M. A. Rodriguez, B. R. Cherry, J. L. Krumhansl, T. M. Nenoff, A. M. Sattler, *Science* **2002**, *297*, 996.
[14] M. Nyman, A. Tripathi, J. B. Parise, R. S. Maxwell, T. M. Nenoff, *J. Am. Chem. Soc.* **2002**, *124*, 1704.
[15] A. Goiffon, E. Philippot, M. Maurin, *Rev. Chim. Miner.* **1980**, *17*, 466.
[16] Crystal data and structure refinement for **1**: $Na_{16}[SiNb_{12}O_{40}]\cdot 4H_2O$. An approximately cubic crystal ($0.015\times0.015\times0.015$ mm) was analyzed by using f scans with a Bruker 6500 SMART platform at ID11 Beamline at ESRF ($\lambda = 0.50915$ Å) at room temperature; cubic system, space-group $P\bar{4}3n$, $a = 20.5185(16)$ Å, $V = 8638.5(12)$ Å^3, $Z = 8$, $\rho_{calcd} = 3.41$ g cm^{-3}, $\mu = 10.42$ mm^{-1}, F(000) = 8272. 34 707 measured reflections, of which 3505 were independent ($R_{int} = 0.049$). Refinement on F^2, 206 parameters refined, Flack parameter $x = 0.108(23)$; $R1 = 0.0503$ for 3313 $F_{obs} > 4\,s(F_{obs})$ and $R1 = 0.0530$ for all 3505 data, $wR2 = 0.1436$, goodness of fit $S = 1.049$. Residual electron density: +2.54/-1.47 e$^-$ Å^{-3}. Hydrogen atoms of water molecules were not located. Structure solution SIR97 (A. Altomare, M. C. Burla, M. Camalli, G. L. Cascarano, C. Giacovazzo, A. Guagliardi, A. G. G. Moliterni, G. Polidori, R. Spagna, *J. Appl. Crystallogr.* **1999**, *32*, 115–119), structure refinement G. M. Sheldrick, SHELXS-97, Programs for Crystal Structure Analysis, University of Göttingen, Göttingen (Germany), **1997**, crystallographic package Wingx 1.64.05 [L. J. Farrugia, *J. Appl. Crystallogr.* **1999**, *32*, 837–838]. Further details of the crystal structure investigation may be obtained from the Fachinformationszentrum Karlsruhe, 76344 Eggenstein-Leopoldshafen, Germany (fax: (+49) 7247–808–666; e-mail: crysdata@fiz-karlsruhe.de) on quoting the depository number CSD-413539).
[17] J. A. Rodriguez-Carvajal, "FULLPROF: A Program for Rietveld Refinement and Pattern Matching Analysis", Abstracts of the Satellite Meeting on Powder Diffraction of the XV Congress of the IUCr, Toulouse, France, **1990**, p. 127.
[18] A. LeBail, H. Duroy, J. L. Fourquet, *Mater. Res. Bull.* **1988**, *23*, 447.
[19] B. E. Brese, M. O'Keefe, *Acta Crystallogr. Sect. B* **1991**, *47*, 192.
[20] G. Engelhardt, D. Michel, John Wiley & Sons, Chichester, **1987**, p. 77.
[21] A. Labouriau, T. J. Higley, W. L. Earl, *J. Phys. Chem.* **1998**, *102*, 2897.
[22] M. Nyman, L. J. Criscenti, F. Bonhomme, M. A. Rodriguez, R. T. Cygan, *J. Solid State Chem.* **2003**, *176*, 111.
[23] C. M. Flynn, G. A. Stucky, *Inorg. Chem.* **1969**, *8*, 335.
[24] E. J. Graeber, B. Morosin, *Acta Crystallogr. Sect. B* **1977**, *33*, 2137.
[25] I. V. Kozhevnikov, A. Sinnema, R. J. J. Jansen, H. vanBekkum, *Mendeleev Commun.* **1994**, *3*, 92.
[26] I. V. Kozhevnikov, A. Sinnema, R. J. J. Jansen, H. vanBekkum, *Catal. Lett.* **1994**, *27*, 187.
[27] I. V. Kozhevnikov, A. Sinnema, H. vanBekkum, M. Fournier, *Catal. Lett.* **1996**, *41*, 153.
[28] M. Filowitz, R. K. C. Ho, W. G. Klemperer, W. Shum, *Inorg. Chem.* **1979**, *18*, 93.
[29] A. E. Bennet, C. M. Rienstra, M. Auger, K. V. Lakshmi, R. G. Griffin, *J. Chem. Phys.* **1995**, *103*, 6951.

